

Relic Abundance of Asymmetric Dark Matter in Quintessence

Hoernisa Iminniyaz^{a*}, Xuelei Chen^{b†}

^a*School of Physics Science and Technology, Xinjiang University,
Urumqi 830046, China*

^b*National Astronomical Observatories, Chinese Academy of Sciences,
Beijing 100012, China*

Abstract

We investigate the relic abundance of asymmetric Dark Matter particles in quintessence model with a kination phase. The analytic calculation of the asymmetric Dark Matter in the standard cosmological scenario is extended to the nonstandard cosmological scenario where we specifically discuss the quintessence model with a kination phase. We found that the enhancement of Hubble rate changes the relic density of particles and anti-particles. We use the present day Dark Matter abundance to constrain the Hubble rate in quintessence model with a kination phase for asymmetric Dark Matter.

arXiv:1308.0353v1 [hep-ph] 1 Aug 2013

*wrns@xju.edu.cn

†xuelei@cosmology.bao.ac.cn

1 Introduction

The cosmological and astrophysical observations showed that the universe contains large amount of Dark Matter. The Dark Matter relic density is determined by Cosmic Microwave Background (CMB) Anisotropy observations with the Wilkinson Microwave Anisotropy Probe (WMAP) as [1],

$$\Omega_{\text{DM}}h^2 = 0.1109 \pm 0.0056, \quad (1)$$

where Ω_{DM} is the Dark Matter (DM) density in unit of the critical density, and $h = 0.710 \pm 0.025$ is the Hubble constant in units of $100 \text{ km sec}^{-1} \text{ Mpc}^{-1}$.

The nature of the Dark Matter is still a challenging questions for scientists though we have a precise measurement of Dark Matter amount. So far, many Dark Matter candidate particles have been proposed beyond the Standard Model (SM). Among them neutral, long-lived or stable weakly interacting massive particles (WIMP) are considered excellent candidates for Dark Matter. Neutralino is one of the most promising candidate for Dark Matter which appears in supersymmetric standard model, neutralino is stabilized due to the conserved R -parity [2]. Neutralino is Majorana particle for which its particle and anti-particle are the same. However this is only one possibility. Most of the known elementary particles in the universe indeed are not Majorana particles, the particles and anti-particles are distinct if we consider fermionic particles. There is one option that assumes the Dark Matter particles can be Dirac particles. The average density of baryons and Dark Matter is comparable. This motivates to consider Dark Matter can be asymmetric particles [3, 4]. [5, 6] investigated the relic abundance of asymmetric Dark Matter particles in the standard cosmological scenario in which particles were in thermal equilibrium in the early universe and decoupled when they were non-relativistic.

On the other hand, the Dark Matter relic density is changed by the modified expansion rate of the universe. The reason for that might be the additional contributions to the total energy density from quintessence model [7], anisotropic expansion [8], a modification of general relativity [8, 9] and etc. In paper by Salati [7], it was shown that the relic density of Dark Matter is increased when the expansion rate of the universe is changed in the quintessence model. There is no discussion about the asymmetric Dark Matter relic density in nonstandard cosmological scenarios including quintessence model until now. It deserves to investigate the relic density of asymmetric Dark Matter in the nonstandard cosmological scenarios and find to what extent the asymmetric Dark Matter relic density is affected by the modification of the Hubble rate.

In this paper, we extend the discussion about the relic density of asymmetric WIMP Dark Matter in the standard cosmological scenario to the nonstandard cosmological scenario,

specifically we examine the asymmetric WIMP Dark Matter relic density in quintessence model with a kination phase. We assume that the Dark Matter asymmetry is created before Dark Matter annihilation reactions freeze-out. In the beginning we assume there are more particles than the anti-particles. We find that the enhanced Hubble rate in quintessence model changes the relic density of both particles and anti-particles. We closely follow the analytic solution of asymmetric Dark Matter in standard cosmological scenario and derived the analytic solution of the relic density of asymmetric Dark Matter in quintessence model.

This paper is arranged as follows. In section 2, we review the relic density of asymmetric Dark Matter in the standard cosmological scenario. In section 3, the relic density of asymmetric Dark Matter in quintessence model with a kination phase is discussed. In section 4, we constrained the expansion rate in quintessence model with a kination phase using the observed Dark Matter abundance. The last section is devoted to the conclusions and discussions.

2 Relic Abundance of Asymmetric Dark Matter in the Standard Cosmological Scenario

In this section, we review the relic abundance of asymmetric Dark Matter in the standard cosmological scenario which assumes particles were in thermal equilibrium in the early universe and decoupled when they were non-relativistic [5]. χ is denoted as a Dark Matter particle that is *not* self-conjugate, i.e. the anti-particle $\bar{\chi} \neq \chi$. Time evolutions of the number densities n_χ , $n_{\bar{\chi}}$ in the expanding universe are described by the Boltzmann equations. Solving Boltzmann equations, we obtain the relic densities of χ and $\bar{\chi}$ particles. It is assumed that only $\chi\bar{\chi}$ pairs can annihilate into Standard Model (SM) particles, while $\chi\chi$ and $\bar{\chi}\bar{\chi}$ pairs can not, the Boltzmann equations are:

$$\begin{aligned} \frac{dn_\chi}{dt} + 3Hn_\chi &= -\langle\sigma v\rangle(n_\chi n_{\bar{\chi}} - n_{\chi,\text{eq}}n_{\bar{\chi},\text{eq}}); \\ \frac{dn_{\bar{\chi}}}{dt} + 3Hn_{\bar{\chi}} &= -\langle\sigma v\rangle(n_\chi n_{\bar{\chi}} - n_{\chi,\text{eq}}n_{\bar{\chi},\text{eq}}), \end{aligned} \quad (2)$$

where $\langle\sigma v\rangle$ is the thermally averaged annihilation cross section multiplied with the relative velocity of the two annihilating χ , $\bar{\chi}$ particles. $H = \dot{R}/R$ is the expansion rate of the universe, where R is the scale factor of the universe. $n_{\chi,\text{eq}}$, $n_{\bar{\chi},\text{eq}}$ are the equilibrium number densities of χ and $\bar{\chi}$, here it is assumed the Dark Matter particles were non-relativistic at decoupling. Then the equilibrium number densities $n_{\chi,\text{eq}}$ and $n_{\bar{\chi},\text{eq}}$ are

$$\begin{aligned} n_{\chi,\text{eq}} &= g_\chi \left(\frac{m_\chi T}{2\pi}\right)^{3/2} e^{(-m_\chi + \mu_\chi)/T}, \\ n_{\bar{\chi},\text{eq}} &= g_\chi \left(\frac{m_\chi T}{2\pi}\right)^{3/2} e^{(-m_\chi - \mu_{\bar{\chi}})/T}, \end{aligned} \quad (3)$$

where m_χ is the mass of the Dark Matter particle χ and $\bar{\chi}$, and g_χ is the number of the internal degrees of freedom of the χ and $\bar{\chi}$ separately. $\mu_\chi, \mu_{\bar{\chi}}$ are the chemical potential of the particles and anti-particles, $\mu_{\bar{\chi}} = -\mu_\chi$ in equilibrium.

At high temperature χ and $\bar{\chi}$ particles are in thermal equilibrium in the early universe. When $T < m_\chi$, for $m_\chi > |\mu_\chi|$, the number densities $n_{\chi,\text{eq}}$ and $n_{\bar{\chi},\text{eq}}$ decrease exponentially. Finally the interaction rates $\Gamma = n_\chi \langle \sigma v \rangle$ and $\bar{\Gamma} = n_{\bar{\chi}} \langle \sigma v \rangle$ drop below H . χ and $\bar{\chi}$ particles are then no longer kept in chemical equilibrium, and their co-moving number densities are fixed. The temperature at which the WIMPs drop out of chemical equilibrium is called the freeze-out temperature.

For convenient, the Boltzmann equations (2) can be rewritten in terms of the dimensionless quantities $Y_\chi = n_\chi/s$, $Y_{\bar{\chi}} = n_{\bar{\chi}}/s$, and $x = m_\chi/T$. The entropy density is given by $s = (2\pi^2/45)g_*sT^3$, where

$$g_*s = \sum_{i=\text{bosons}} g_i \left(\frac{T_i}{T} \right)^3 + \frac{7}{8} \sum_{i=\text{fermions}} g_i \left(\frac{T_i}{T} \right)^3. \quad (4)$$

Here g_i is equivalent to g_χ , T_i is the temperature of species i . During the radiation-dominated epoch, the expansion rate H is given by

$$H = \frac{\pi T^2}{M_{\text{Pl}}} \sqrt{\frac{g_*}{90}}, \quad (5)$$

with $M_{\text{Pl}} = 2.4 \times 10^{18}$ GeV being the reduced Planck mass and

$$g_* = \sum_{i=\text{bosons}} g_i \left(\frac{T_i}{T} \right)^4 + \frac{7}{8} \sum_{i=\text{fermions}} g_i \left(\frac{T_i}{T} \right)^4. \quad (6)$$

It is assumed that the universe expands adiabatically during this period, then the Boltzmann equations (2) become

$$\frac{dY_\chi}{dx} = -\frac{\lambda \langle \sigma v \rangle}{x^2} (Y_\chi Y_{\bar{\chi}} - Y_{\chi,\text{eq}} Y_{\bar{\chi},\text{eq}}); \quad (7)$$

$$\frac{dY_{\bar{\chi}}}{dx} = -\frac{\lambda \langle \sigma v \rangle}{x^2} (Y_\chi Y_{\bar{\chi}} - Y_{\chi,\text{eq}} Y_{\bar{\chi},\text{eq}}), \quad (8)$$

where

$$\lambda = 1.32 m_\chi M_{\text{Pl}} \sqrt{g_*}. \quad (9)$$

Here we assume $g_* \simeq g_{*s}$ and $dg_*/dx \simeq 0$.

Subtracting Eq.(7) from Eq.(8),

$$\frac{dY_\chi}{dx} - \frac{dY_{\bar{\chi}}}{dx} = 0. \quad (10)$$

This indicate

$$Y_\chi - Y_{\bar{\chi}} = C, \quad (11)$$

where C is a constant, the difference of the co-moving densities of the particles and anti-particles is conserved. Expressing Eqs.(7) and (8) using Eq.(11), the Boltzmann equations become

$$\frac{dY_\chi}{dx} = -\frac{\lambda\langle\sigma v\rangle}{x^2} (Y_\chi^2 - CY_\chi - P); \quad (12)$$

$$\frac{dY_{\bar{\chi}}}{dx} = -\frac{\lambda\langle\sigma v\rangle}{x^2} (Y_{\bar{\chi}}^2 + CY_{\bar{\chi}} - P), \quad (13)$$

where

$$P = Y_{\chi,\text{eq}}Y_{\bar{\chi},\text{eq}} = (0.145g_\chi/g_*)^2 x^3 e^{-2x}. \quad (14)$$

Usually the WIMP annihilation cross section can be expanded in the relative velocity v between the annihilating WIMPs. Its thermal average is given by

$$\langle\sigma v\rangle = a + 6bx^{-1} + \mathcal{O}(x^{-2}). \quad (15)$$

Here a is s -wave contribution to σv while $b = 0$, and b is p -wave contribution to σv while $a = 0$.

In the standard cosmological scenario, the following approximate formulae are obtained for the relic abundances of particles and anti-particles:

$$Y_\chi(x \rightarrow \infty) = \frac{C}{1 - \exp[-1.32 C m_\chi M_{\text{Pl}} \sqrt{g_*} (ax_F^{-1} + 3bx_F^{-2})]}, \quad (16)$$

$$Y_{\bar{\chi}}(x \rightarrow \infty) = \frac{C}{\exp[1.32 C m_\chi M_{\text{Pl}} \sqrt{g_*} (a \bar{x}_F^{-1} + 3b \bar{x}_F^{-2})] - 1}, \quad (17)$$

where we have used Eq.(9). x_F and \bar{x}_F are the inverse scaled freeze-out temperatures of χ and $\bar{\chi}$. Eqs.(16) and (17) are only consistent with the constraint (11) if $x_F = \bar{x}_F$. For convenience, the final abundance is expressed as

$$\Omega_\chi h^2 = \frac{m_\chi s_0 Y_\chi(x \rightarrow \infty) h^2}{\rho_{\text{crit}}}, \quad (18)$$

where $s_0 = 2.9 \times 10^3 \text{ cm}^{-3}$ is the present entropy density, and $\rho_{\text{crit}} = 3M_{\text{Pl}}^2 H_0^2$ is the present critical density. The corresponding prediction for the present relic density for Dark Matter is given by

$$\Omega_{\text{DM}} h^2 = 2.76 \times 10^8 m_\chi [Y_\chi(x \rightarrow \infty) + Y_{\bar{\chi}}(x \rightarrow \infty)] \text{ GeV}^{-1}. \quad (19)$$

We defer further discussions of this expression to Sec.3 where the asymmetric Dark Matter relic density in the quintessence model with a kination phase is analyzed.

3 Relic Abundance of WIMPs in Quintessence

Before going to the discussion of the relic density in quintessence model with a kination phase, let us briefly review the model. A kination is a period in which the kinetic energy of a scalar field $\rho_\phi \simeq \dot{\phi}^2/2$ dominates over the potential energy density $V(\phi)$ and the radiation energy density ρ_{rad} . A kination phase is appeared in quintessence models based on tracking solutions for the scalar field [7]. The overall energy density decreases as $\rho_{tot} \simeq \dot{\phi}^2/2 \sim R^{-6}$. $T \sim R^{-1}$, thus $H^2 \sim \rho_{tot} \sim T^6$. It means H decreases faster as T decreases or H decreases faster as the scale factor R increases. The ratio of the expansion rate H during kination period and the expansion rate of the standard case H_{std} is given by:

$$\frac{H^2}{H_{std}^2} = 1 + \frac{\rho_\phi}{\rho_r}, \quad (20)$$

where the ratio of the scalar energy density to the radiation energy density ρ_ϕ/ρ_r is [7]

$$\frac{\rho_\phi}{\rho_r} = \eta \left[\frac{g_{*s}(T)}{g_{*s}(T_0)} \right]^2 \frac{g_*(T_0)}{g_*(T)} \left(\frac{T}{T_0} \right)^2 \simeq \eta \left(\frac{T}{T_0} \right)^2, \quad (21)$$

where $\eta = \rho_\phi(T_0)/\rho_r(T_0)$. Here T_0 is some reference temperature which is close to the freeze-out temperature. The approximation of the above equation only holds in a range of temperatures where g_{*s} and g_* do not change sizably with respect to their value at T_0 . We can rewrite Eq.(20) as

$$H = A(T)H_{std}, \quad (22)$$

where the enhancement function $A(T)$ is

$$A(T) = \sqrt{1 + \eta \left(\frac{T}{T_0} \right)^2}. \quad (23)$$

In order not to spoil the successful prediction of Big Bang Nucleosynthesis BBN, $A(T)$ must return to 1 at the low temperature around 1 MeV. With the modified expansion rate, the Boltzmann Eqs.(12), (13) become

$$\frac{dY_\chi}{dx} = -\frac{\lambda\langle\sigma v\rangle}{x^2 A(x)} (Y_\chi^2 - CY_\chi - P); \quad (24)$$

$$\frac{dY_{\bar{\chi}}}{dx} = -\frac{\lambda\langle\sigma v\rangle}{x^2 A(x)} (Y_{\bar{\chi}}^2 + CY_{\bar{\chi}} - P). \quad (25)$$

Fig.1 is obtained by the numerical solutions of Eqs.(24), (25) for the different values of the enhancement factor η with different asymmetry factor C . The solid (red) line is the equilibrium value of the anti-particle abundance. The double dotted (black) line is for the anti-particle

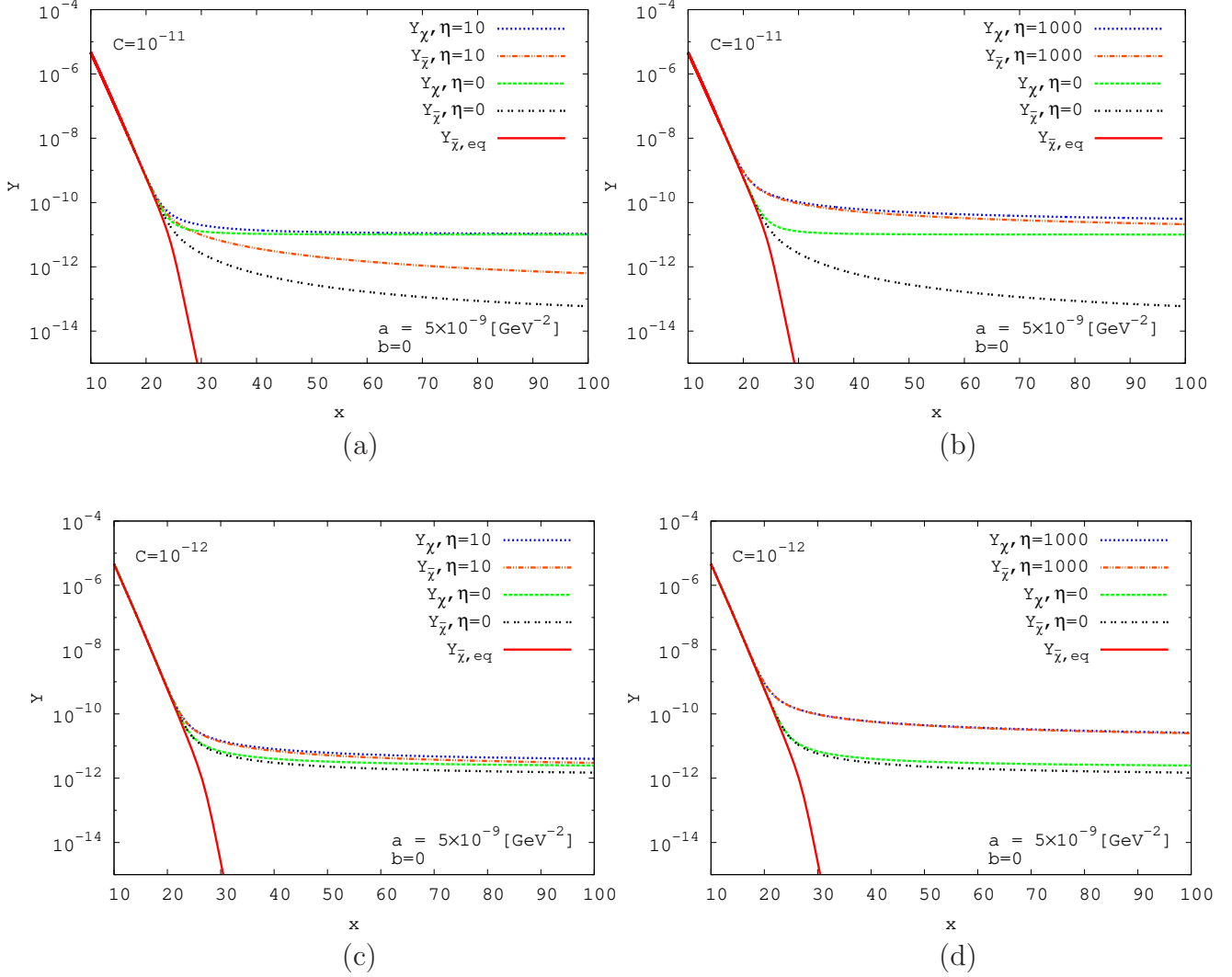


Figure 1: The relic abundances Y_χ and $Y_{\bar{\chi}}$ for particle χ and anti-particle $\bar{\chi}$ as a function of the inverse-scaled temperature for $\eta = 10$ (a), (c) and $\eta = 1000$ (b), (d). Here we take $a = 5.0 \times 10^{-9} \text{ GeV}^{-2} = 5.9 \times 10^{-26} \text{ cm}^3 \text{ s}^{-1}$, $b = 0$, $m = 100 \text{ GeV}$, $x_0 = 20$, $C = 10^{-11}$ for (a) and (b), $C = 10^{-12}$ for (c) and (d)

abundance and the dashed (green) line is for particle abundance in the standard scenario ($\eta = 0$). The dot-dashed (red) line is for the abundance of anti-particle and dotted (blue) line is for abundance of particle for $\eta = 10$ left (a), (c) frames and $\eta = 1000$ right (b), (d) frames. In [10, 11, 12], the authors found the constraints for η as $\eta < 10^6$ for the WIMPs mass $m_\chi < 1 \text{ TeV}$. We discuss the asymmetric WIMPs mass $m_\chi < 1 \text{ TeV}$. Therefore, we take $\eta = 10$ and $\eta = 1000$ for examples. Here we take $C = 10^{-11}$, for (a), (b) and $C = 10^{-12}$ for (c), (d), $m_\chi = 100 \text{ GeV}$, $a = 5.0 \times 10^{-9} \text{ GeV}^{-2} = 5.9 \times 10^{-26} \text{ cm}^3 \text{ s}^{-1}$, $b = 0$, $g_\chi = 2$ and $g_* = 90$, $x_0 = 20$, where $x_0 = m/T_0$.

The relic abundances Y_χ and $Y_{\bar{\chi}}$ for particle χ and anti-particle $\bar{\chi}$ are increased in Fig.1 (a), (c) frames for $\eta = 10$ and (b), (d) frames for $\eta = 1000$. The expansion rate is enhanced in

quintessence model with a kination phase. The particles and anti-particles freeze-out earlier than the standard case. This leads to the increases of particle and anti-particle abundances. As we noted in introduction, we assume there are more particles than the anti-particles. For smaller η ($\eta = 10$, (a), (c) left frames), the relic abundances for particles and anti-particles are not affected too much. When η is large ($\eta = 1000$, (b), (d) right frames), the relic abundances for particles and anti-particles are increased significantly. In frames (a), (b), the relic abundance of anti-particle seems to be increased more sizably than the particle relic abundance for the asymmetry factor $C = 10^{-11}$. In fact there are same increases for particle and anti-particle relic abundances. The reason is the following: let's closely look at the left (a) frame of Fig.1. The anti-particle relic abundance $Y_{\bar{\chi}}$ is 8.0×10^{-14} for $\eta = 0$. It is increased to 8.0×10^{-13} for $\eta = 10$. It is one order increase. According to Eq.(11), $Y_{\chi} = Y_{\bar{\chi}} + C$, here $C = 10^{-11}$. Thus the particle χ abundance is increased almost 10% for $\eta = 10$. This is only small deviation. On the other hand, when the asymmetry factor C is small ($C = 10^{-12}$), the increases for particles and anti-particles are comparable which are shown in frames (c) and (d) in Fig.1.

Following [5], we obtain the analytic solution of the relic density for asymmetric Dark Matter in quintessence model with a kination phase. First, we solve Eq.(25) for $\bar{\chi}$ density, then χ density can be computed trivially using Eq.(11). We introduce the quantity $\Delta_{\bar{\chi}} = Y_{\bar{\chi}} - Y_{\bar{\chi},\text{eq}}$. In terms of $\Delta_{\bar{\chi}}$, the Boltzmann equation (25) can be rewritten as:

$$\frac{d\Delta_{\bar{\chi}}}{dx} = -\frac{dY_{\bar{\chi},\text{eq}}}{dx} - \frac{\lambda\langle\sigma v\rangle}{x^2 A(x)} [\Delta_{\bar{\chi}}(\Delta_{\bar{\chi}} + 2Y_{\bar{\chi},\text{eq}}) + C\Delta_{\bar{\chi}}]. \quad (26)$$

The solution of this equation can be considered in two regimes. At sufficiently high temperature, $Y_{\bar{\chi}}$ tracks its equilibrium value $Y_{\bar{\chi},\text{eq}}$ very closely. In that regime $\Delta_{\bar{\chi}}$ is small, and $d\Delta_{\bar{\chi}}/dx$ and $\Delta_{\bar{\chi}}^2$ are negligible. The Boltzmann equation (26) then becomes

$$\frac{dY_{\bar{\chi},\text{eq}}}{dx} = -\frac{\lambda\langle\sigma v\rangle}{x^2 A(x)} (2\Delta_{\bar{\chi}}Y_{\bar{\chi},\text{eq}} + C\Delta_{\bar{\chi}}). \quad (27)$$

We need an explicit expression for the equilibrium density $Y_{\bar{\chi},\text{eq}}(x)$ to solve Eq.(27). The right-hand sides of the Boltzmann equations (7) and (8) vanish in equilibrium by definition. Hence the right-hand side of Eq.(25) should vanish as well for $Y_{\bar{\chi}} = Y_{\bar{\chi},\text{eq}}$, which implies

$$Y_{\bar{\chi},\text{eq}}^2 + CY_{\bar{\chi},\text{eq}} - P = 0. \quad (28)$$

There are two solutions for the quadratic equation, only one of them yields a positive $\bar{\chi}$ equilibrium density:

$$Y_{\bar{\chi},\text{eq}} = -\frac{C}{2} + \sqrt{\frac{C^2}{4} + P}. \quad (29)$$

Eq.(29) is inserted into Eq.(27) and ignoring x relative to x^2 , we have

$$\Delta_{\bar{\chi}} \simeq \frac{2x^2 A(x) P}{\lambda \langle \sigma v \rangle (C^2 + 4P)}. \quad (30)$$

We will use this solution to determine the freeze-out temperature \bar{x}_F for $\bar{\chi}$.

When the temperature is sufficiently low, i.e. for $x > \bar{x}_F$, the production term $\propto Y_{\bar{\chi},\text{eq}}$ can be ignored in the Boltzmann equation (26), so that

$$\frac{d\Delta_{\bar{\chi}}}{dx} = -\frac{\lambda \langle \sigma v \rangle}{x^2 A(x)} (\Delta_{\bar{\chi}}^2 + C \Delta_{\bar{\chi}}). \quad (31)$$

Integrating Eq.(31) from \bar{x}_F to ∞ and assuming $\Delta_{\bar{\chi}}(\bar{x}_F) \gg \Delta_{\bar{\chi}}(\infty)$, we have

$$Y_{\bar{\chi}}(x \rightarrow \infty) = \frac{C}{\exp [1.32 C m_{\chi} M_{\text{Pl}} \sqrt{g_*} I(\bar{x}_F)] - 1}, \quad (32)$$

here

$$I(\bar{x}_F) = \int_{\bar{x}_F}^{\infty} \frac{\langle \sigma v \rangle}{x^2 A(x)} dx \quad (33)$$

$$= \frac{a}{\sqrt{\eta} x_0} \ln \left(\sqrt{\eta} \frac{x_0}{\bar{x}_F} + \sqrt{1 + \eta \frac{x_0^2}{\bar{x}_F^2}} \right) + \frac{6b}{\eta x_0^2} \left(\sqrt{1 + \eta \frac{x_0^2}{\bar{x}_F^2}} - 1 \right). \quad (34)$$

Using equation (11), we obtain the relic abundance for χ particle. The result is

$$Y_{\chi}(x \rightarrow \infty) = \frac{C}{1 - \exp [-1.32 C m_{\chi} M_{\text{Pl}} \sqrt{g_*} I(x_F)]}, \quad (35)$$

where $I(x_F)$ is given by

$$I(x_F) = \int_{x_F}^{\infty} \frac{\langle \sigma v \rangle}{x^2 A(x)} dx \quad (36)$$

$$= \frac{a}{\sqrt{\eta} x_0} \ln \left(\sqrt{\eta} \frac{x_0}{x_F} + \sqrt{1 + \eta \frac{x_0^2}{x_F^2}} \right) + \frac{6b}{\eta x_0^2} \left(\sqrt{1 + \eta \frac{x_0^2}{x_F^2}} - 1 \right). \quad (37)$$

Here Eqs.(32) and (35) are only consistent with the constraint (11) if $x_F = \bar{x}_F$. The prediction for the present relic density for Dark Matter is then given by

$$\Omega_{\text{DM}} h^2 = \frac{2.76 \times 10^8 m_{\chi} C}{\exp [1.32 C m_{\chi} M_{\text{Pl}} \sqrt{g_*} I(\bar{x}_F)] - 1} + \frac{2.76 \times 10^8 m_{\chi} C}{1 - \exp [-1.32 C m_{\chi} M_{\text{Pl}} \sqrt{g_*} I(x_F)]}. \quad (38)$$

When $A(x) = 1$, the standard result for asymmetric Dark Matter is recovered. The freeze-out temperature for $\bar{\chi}$ is fixed by assuming that freeze-out occurs when the deviation $\Delta_{\bar{\chi}}$ is of the same order of the equilibrium value of $Y_{\bar{\chi}}$:

$$\xi Y_{\bar{\chi},\text{eq}}(\bar{x}_{F_0}) = \Delta_{\bar{\chi}}(\bar{x}_{F_0}), \quad (39)$$

where ξ is a numerical constant of order unity, $\xi = \sqrt{2} - 1$ [13]. \bar{x}_{F_0} is the freeze-out temperature which is calculated from Eq.(39) using the standard approximation. We found the standard treatment under-predicts the $\bar{\chi}$ relic density. Therefore, the correction is made for the freeze-out temperature as following:

$$\bar{x}_F = \bar{x}_{F_0} \left[1 + \frac{\lambda C}{A(\bar{x}_{F_0})} \left(\frac{0.285a}{\bar{x}_{F_0}^3} + \frac{1.350b}{\bar{x}_{F_0}^4} \right) \right]. \quad (40)$$

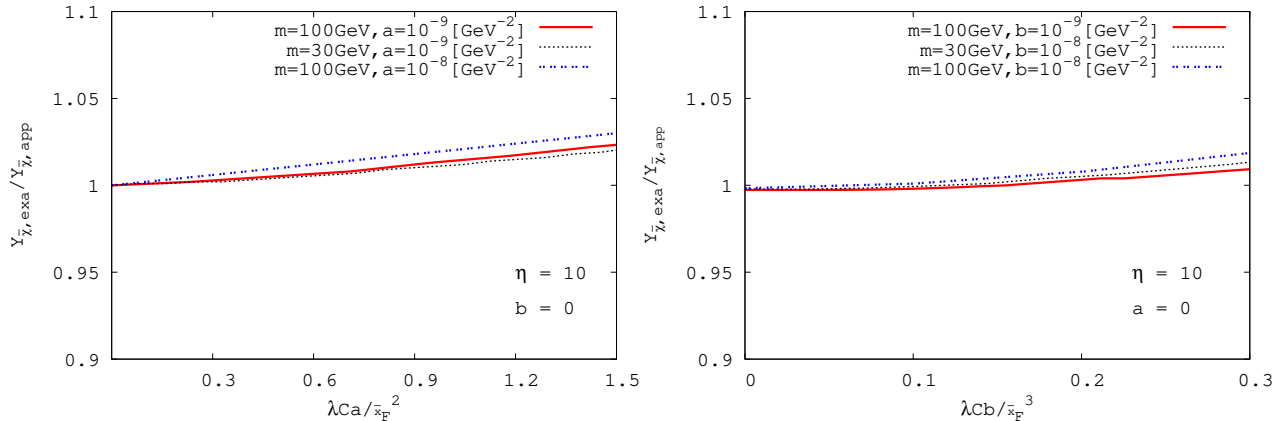


Figure 2: The ratio of the exact value of the $\bar{\chi}$ particle abundance to the analytic value of $\bar{\chi}$ particle abundance for $\eta = 10$ (a) $b = 0$ and (b) $a = 0$, $x_0 = 20$.

The ratio of the exact value of the $\bar{\chi}$ particle abundance to our analytical approximation is plotted in Fig.2 for quintessence model with a kination phase. For $\lambda Ca/x_F^2 \lesssim 1.5$ ($\lambda Cb/x_F^3 \lesssim 0.3$), the approximate analytic result matches the exact numerical result very well, our approximation reproduces the exact numerical solution to better than 3% (2%) for $\eta = 10$.

4 Constraints on Parameter Space

The Dark Matter density is derived as in Eq.(1) by WMAP team using the CMB data for the minimal Λ CDM model. We use this result to find the constraints on the enhancement factor η in the quintessence model with a kination phase. We use the following range for Dark Matter relic density,

$$0.10 < \Omega_{\text{DM}} h^2 < 0.12 \quad (41)$$

The total Dark Matter density should be the addition of the particle χ and anti-particle $\bar{\chi}$ contributions:

$$\Omega_{\text{DM}} = \Omega_{\chi} + \Omega_{\bar{\chi}}. \quad (42)$$

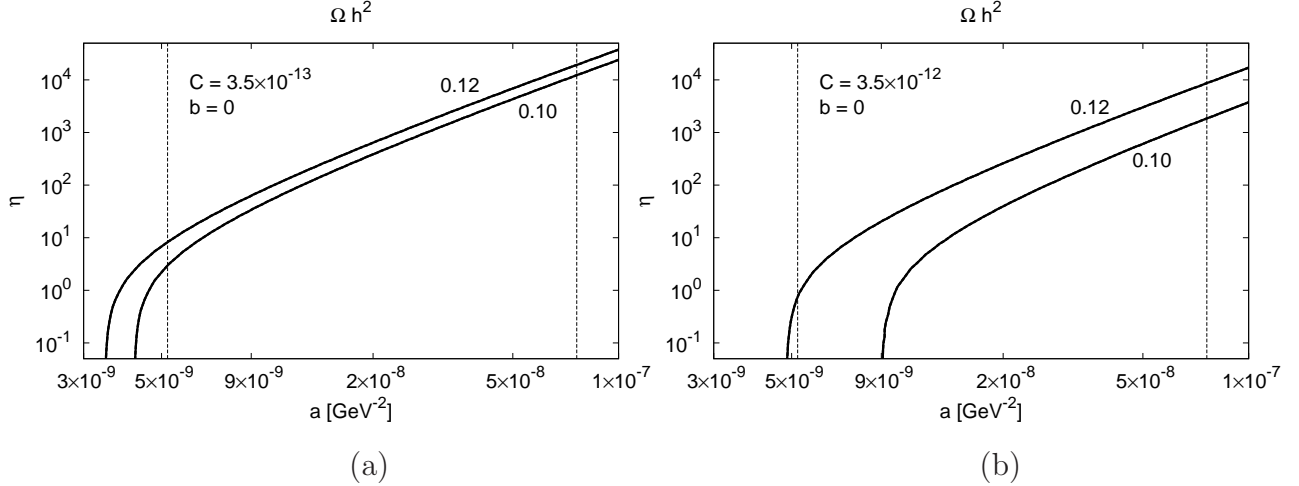


Figure 3: The allowed region in the (a, η) plane for $b = 0$, when the Dark Matter density Ωh^2 lies between 0.10 and 0.12. Here we take $m_\chi = 100$ GeV, $g_\chi = 2$ and $g_* = 90$, $x_0 = 20$; $C = 3.5 \times 10^{-13}$ for (a) and $C = 3.5 \times 10^{-12}$ for (b). The two vertical lines $6.0 \times 10^{-26} \text{ cm}^3 \text{ s}^{-1} = 5.2 \times 10^{-9} \text{ GeV}^{-2}$ and $8.8 \times 10^{-25} \text{ cm}^3 \text{ s}^{-1} = 7.6 \times 10^{-8} \text{ GeV}^{-2}$ are the upper limits for the cross sections for mass 100 GeV from the *Fermi*-LAT collaboration [14].

Fig.3 shows the relation between the s-wave annihilation cross section parameter a and the enhancement factor η for two values of the total Dark Matter density. This figure is based on the exact numerical solutions of Boltzmann equations (24), (25). We use the annihilation cross section which is given by Eq.(15). Here we take $m_\chi = 100$ GeV, $g_\chi = 2$ and $g_* = 90$, $x_0 = 20$; $C = 3.5 \times 10^{-13}$ for (a) and $C = 3.5 \times 10^{-12}$ for (b). We choose such values for asymmetry factor C which are in the range of the values to obtain the observed Dark Matter abundance [5].

In [10, 11, 12], the authors found that the maximal density enhancement compatible with BBN bounds is of the order of 10^6 (for WIMP mass smaller than 1 TeV). In our work we used the observed Dark Matter abundance and derived constraints on η when the asymmetry factor C is fixed. In the left frame of Fig.3, for small asymmetry factor $C = 3.5 \times 10^{-13}$, it is shown that for the values of s-wave annihilation cross sections from $a = 3.6 \times 10^{-9} \text{ GeV}^{-2}$ to $a = 1.0 \times 10^{-7} \text{ GeV}^{-2}$, the observed Dark Matter abundance is obtained for the range of η from 5.0×10^{-2} to 3.8×10^4 . In the right frame of Fig.3, for the asymmetry factor $C = 3.5 \times 10^{-12}$, one needs the s-wave annihilation cross sections from $a = 4.8 \times 10^{-9} \text{ GeV}^{-2}$ to $a = 1.0 \times 10^{-7} \text{ GeV}^{-2}$ in the range of η from 5.0×10^{-2} to 1.5×10^4 to obtain the observed Dark Matter abundance. The annihilation cross section constraints are in the range of the limit which are given by *Fermi*-LAT collaboration [14]. *Fermi*-LAT collaboration [14] gives the upper limit on the cross section from about $10^{-26} \text{ cm}^3 \text{ s}^{-1} = 8.6 \times 10^{-10} \text{ GeV}^{-2}$ at 5 GeV to about $5 \times 10^{-23} \text{ cm}^3 \text{ s}^{-1} = 4.3 \times 10^{-6} \text{ GeV}^{-2}$ at 1 TeV. For $m_\chi = 100$ GeV, the limit from

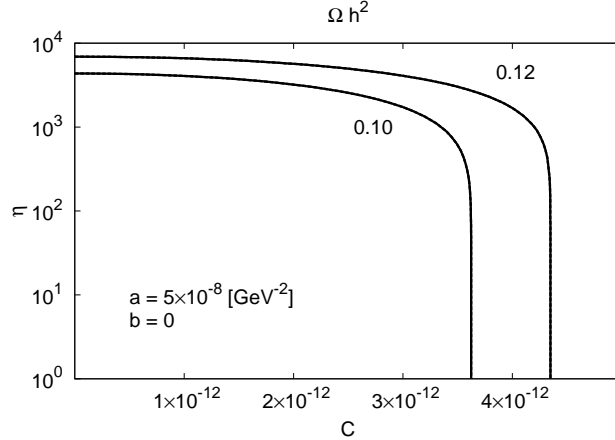


Figure 4: The allowed region in the (η, C) plane for $a = 5 \times 10^{-8} \text{ GeV}^{-2}$, $b = 0$, when the Dark Matter density Ωh^2 lies between 0.10 and 0.12. Here we take $m_\chi = 100 \text{ GeV}$, $g_\chi = 2$ and $g_* = 90$, $x_0 = 20$.

Fermi-LAT collaboration [14] is $6.0 \times 10^{-26} \text{ cm}^3 \text{ s}^{-1} = 5.2 \times 10^{-9} \text{ GeV}^{-2}$ to $8.8 \times 10^{-25} \text{ cm}^3 \text{ s}^{-1} = 7.6 \times 10^{-8} \text{ GeV}^{-2}$.

Fig.4 shows the allowed region in the (η, C) plane for $a = 5 \times 10^{-8} \text{ GeV}^{-2}$, $b = 0$, when the Dark Matter density $\Omega_{\text{DM}} h^2$ lies between 0.10 and 0.12. Here we take $m_\chi = 100 \text{ GeV}$, $g_\chi = 2$ and $g_* = 90$, $x_0 = 20$. When the asymmetry factor C ranges from $C = 0$ to $C = 3.6 \times 10^{-12}$, η should be around $\eta = 7.5 \times 10^2$ to $\eta = 8.0 \times 10^3$ to obtain the observed Dark Matter relic density. η is not sensitive to the asymmetry factor in this case. In contrast for asymmetry factor which ranges from $C = 3.6 \times 10^{-12}$ to $C = 4.3 \times 10^{-12}$, η is from $\eta = 1$ to $\eta = 7.5 \times 10^2$ to obtain the observed Dark Matter abundance.

5 Summary and Conclusions

In this paper we investigated the relic abundance of asymmetric WIMP Dark Matter in quintessence model with a kination phase. The Dark Matter particles and anti-particles are distinct in the asymmetric Dark Matter Scenario. We assume the asymmetry starts well before the epoch of thermal decoupling of the WIMPs. In quintessence model with a kination phase, the asymmetric Dark Matter particles freeze-out earlier than the standard case due to the enhanced Hubble rate. This leads to the increase of the relic density of asymmetric Dark Matter particles. We treat the enhancement factor η and asymmetry factor C as free parameters in our work.

The discussion of the relic density of asymmetric Dark Matter in the standard cosmological scenario which assumes the particles were in thermal equilibrium in the early universe and decoupled when they were non-relativistic has been done in paper [5, 6]. In our work, we

extend it to the nonstandard cosmological scenario where the Hubble rate of the universe is changed in quintessence model. We investigated the relic density of asymmetric WIMP Dark Matter in this model. Using the observed Dark Matter abundance, we find the constraints on the enhancement factor η assuming the asymmetry factor C is fixed.

We found that the relic densities of both particles and anti-particles are increased in quintessence model with a kination phase. The size of the increase depends on the enhancement factor η . For the large enhancement factor η , the increases are more sizable than the smaller enhancement factor η .

For the range of cross section $a = 3.6 \times 10^{-9} \text{ GeV}^{-2}$ to $a = 1.0 \times 10^{-7} \text{ GeV}^{-2}$, one needs the enhancement factor η from 5.0×10^{-2} to 3.8×10^4 for $C = 3.5 \times 10^{-13}$ to obtain the observed relic density of asymmetric Dark Matter. When $C = 3.5 \times 10^{-12}$, the observed Dark Matter abundance is obtained for the enhancement factor η from 5.0×10^{-2} to 1.5×10^4 for the cross sections from $a = 4.8 \times 10^{-9} \text{ GeV}^{-2}$ to $a = 1.0 \times 10^{-7} \text{ GeV}^{-2}$.

Our result is important to understand the relic abundance of asymmetric Dark Matter in the early universe before Big Bang Nucleosynthesis starts. From the observation we can also have constraints on the parameter space for nonstandard cosmological model in asymmetric Dark Matter case. In quintessence model with a kination phase, the abundance of Dark matter and anti-Dark Matter particles are increased.

Note added: as we were revising this manuscript, [15] was appeared, in which the asymmetric dark matter relic density is discussed in nonstandard cosmological scenarios including quintessence model with a kination phase and scalar-tensor model. While the general ideas are similar, the details of the treatment are different, in our work we only concentrated on the quintessence model with a kination phase. For the kination model, our results are in general agreement with theirs.

Acknowledgments

We thank professor Bi Xiao-jun and Shan-Chung Lin for useful discussions. The work is supported by the National Natural Science Foundation of China (11047009) and by the doctor fund BS100108 of Xinjiang university.

References

- [1] N. Jarosik *et al.*, *Astrophys. J. Suppl.* **192**, 14 (2011) E. Komatsu *et al.*, *Astrophys. J. Suppl.* **192**, 18 (2011)

- [2] For a review, see G. Bertone, D. Hooper and J. Silk, Phys. Rep. **405**, 279 (2005) [hep-ph/0404175]; G. Jungman, M. Kamionkowski, and K. Griest, Phys. Rep. **267**, 195 (1996)
- [3] S. Nussinov, Phys. Lett. B **165**, 55 (1985); K. Griest and D. Seckel. Nucl. Phys. B **283**, 681 (1987); R.S. Chivukula and T.P. Walker, Nucl. Phys. B **329**, 445 (1990); D.B. Kaplan, Phys. Rev. Lett. **68**, 742 (1992); D. Hooper, J. March-Russell and S.M. West, Phys. Lett. B **605**, 228 (2005) [arXiv:hep-ph/0410114]; JCAP **0901** (2009) 043 [arXiv:0811.4153v1 [hep-ph]]; H. An, S.L. Chen, R.N. Mohapatra and Y. Zhang, JHEP **1003**, 124 (2010) [arXiv:0911.4463 [hep-ph]]; T. Cohen and K.M. Zurek, Phys. Rev. Lett. **104**, 101301 (2010) [arXiv:0909.2035 [hep-ph]]. D.E. Kaplan, M.A. Luty and K.M. Zurek, Phys. Rev. D **79**, 115016 (2009) [arXiv:0901.4117 [hep-ph]]; T. Cohen, D.J. Phalen, A. Pierce and K.M. Zurek, Phys. Rev. D **82**, 056001 (2010) [arXiv:1005.1655 [hep-ph]]; J. Shelton and K.M. Zurek, Phys. Rev. D **82**, 123512 (2010) [arXiv:1008.1997 [hep-ph]];
- [4] A. Belyaev, M. T. Frandsen, F. Sannino and S. Sarkar, Phys. Rev. D **83**, 015007 (2011) [arXiv:1007.4839].
- [5] H. Iminniyaz, M. Drees and X. Chen, JCAP **1107**, 003 (2011) [arXiv:1104.5548 [hep-ph]].
- [6] M. L. Graesser, I. M. Shoemaker and L. Vecchi, JHEP **1110**, 110 (2011) [arXiv:1103.2771 [hep-ph]].
- [7] P. Salati, Phys. Lett. B **571**, 121 (2003) [astro-ph/0207396].
- [8] M. Kamionkowski and M.S. Turner, Phys. Rev. D **42**, 3310 (1990).
- [9] R. Catena, N. Fornengo, A. Masiero, M. Pietroni and F. Rosati, Phys. Rev. D **70**, 063519 (2004) [arXiv:astro-ph/0403614].
- [10] M. Schelke, R. Catena, N. Fornengo, A. Masiero and M. Pietroni, Phys. Rev. D **74** (2006) 083505 [hep-ph/0605287].
- [11] F. Donato, N. Fornengo and M. Schelke, JCAP **0703**, 021 (2007) [hep-ph/0612374].
- [12] R. Catena, N. Fornengo, M. Pato, L. Pieri and A. Masiero, Phys. Rev. D **81**, 123522 (2010) [arXiv:0912.4421 [astro-ph.CO]].
- [13] R.J. Scherrer and M.S. Turner, Phys. Rev. D **33**, 1585 (1986), Erratum-ibid. D **34**, 3263 (1986); P. Gondolo and G. Gelmini, Nucl. Phys. B **360**, 145 (1991).
- [14] M. Ackermann *et al.* [Fermi-LAT Collaboration], Phys. Rev. Lett. **107**, 241302 (2011) [arXiv:1108.3546 [astro-ph.HE]].
- [15] G. B. Gelmini, J. -H. Huh and T. Rehagen, arXiv:1304.3679 [hep-ph].